

# DESIGN AND MANUFACTURING OF THE NEXT GENERATION OF CERN'S NORTH AREA SPLITTER COLLIMATORS (TCSC)

J. Braken\*, J.L. Grenard†, N. Solieri‡, P.R. Menachilis, A. Romero Francia, M. Timmins, P. Schneider, T. Coiffet, G. Mazzola, D. Wasik, L.S. Esposito, D. Grenier, B. Pittet, M. Fraser, A. Gorn, I. Prieto Rivero, T. Parmentier, A. Perillo Marcone, M. Calviani  
CERN, Geneva, Switzerland

## Abstract

CERN's Transfer Tunnel 20 (TT20) connects the Super Proton Synchrotron (SPS) to three primary targets in the North Area which provide secondary particles to experiments further downstream. Two splitter collimators (TCSC) are installed along this line, each protecting their respective downstream Lambertson septum magnets, which distribute the slow-extracted 400 GeV/c proton beams among the targets. During Long Shutdown 3 (LS3, 2026–2029), two redesigned TCSCs will be installed to improve cooling efficiency, mechanical robustness, and maintainability in the context of the North Area Consolidation (NA CONS) project. The new design also incorporates additional radiation shielding to reduce dose rates in the surrounding area and minimise personnel exposure during tunnel interventions. This contribution presents the main design improvements, thermo-mechanical analyses, and manufacturing developments implemented to enhance the reliability, radiation safety, and thermal performance of the TT20 splitter collimators.

## INTRODUCTION

CERN's North Area beamlines use slow extraction from the Super Proton Synchrotron (SPS) to deliver 400 GeV/c proton beams to multiple targets, providing secondary beams for downstream experiments [1]. Two sets of Lambertson septum magnets (MSSB) split the vertically blown up beam over the branched primary beam lines. A TCSC (Target Collimator Splitter version C) installed upstream of each MSSB, intercepts part of the beam to protect the septum from direct beam impact [2]. Each currently installed TCSC consists of two CuCr1Zr absorber blocks enclosed in a vacuum tank. When clamped together, the absorber blocks form two internal beam apertures that replicate the shape of the splitter magnet yoke located downstream. The separation between both TCSC apertures is formed by a pair of symmetrical wedges, which absorb the portion of the beam that would otherwise strike the MSSB septum, see Fig. 1. The energy deposited by this intercepted beam fraction is converted into heat within the TCSC core. The absorber blocks are water-cooled to dissipate heat caused by the absorbed beam energy.

\* Jules.Johannes.Braken@cern.ch

† Jean-Louis.Grenard@cern.ch

‡ Nicola.Solieri@cern.ch

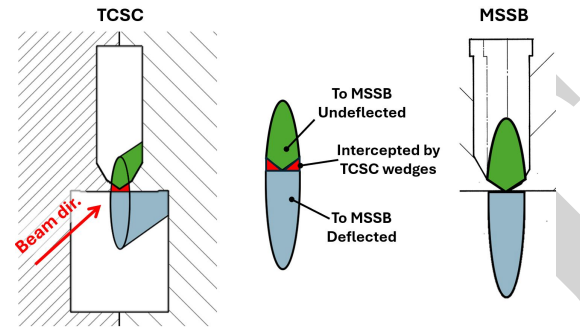


Figure 1: Left: Diagram of beam position with respect to the TCSC cross section. Right: Diagram of nominal beam position with respect to the MSSB septum.

## History

The first pair of TCSCs was built and installed in the late 1970s during the construction of the North Area. Since their installation, one of the devices has been subject to significant corrosion because of a corrosive liquid leak onto its vacuum tank, leading to its replacement by a spare device. As a result of high radiation levels generated by beam impact onto the absorber coupled with its unshielded vacuum tank, water connections have aged and failed during the operation of these devices, leading to high radiation doses received by personnel during replacement interventions.

## DESIGN IMPROVEMENTS

Two redesigned TCSCs will be installed during Long Shutdown 3 (2026–2029) [3]. Their design aims to improve the device robustness and reliability while limiting potential downtime and minimising radiation dose to personnel during interventions. The upgraded CuCr1Zr core retains the initial design idea, consisting of two water-cooled absorber blocks that are bolted together, each maintaining their wedge profile capable of intercepting a portion of the high energy beam, see Fig. 2.

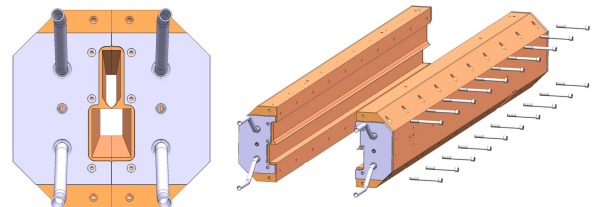


Figure 2: Left: Front view of the TCSC core assembly. Right: The two water-cooled CuCr1Zr blocks are bolted together to form the TCSC core.

The core assembly is housed within a seamless 2.5 m long, radially forged stainless-steel 304L cylindrical vacuum vessel. To minimise radiation dose to personnel during interventions, the vacuum tank is surrounded by a marble external radiation shielding. Additional measures to reduce personnel radiation exposure include improved accessibility of the external water connections that facilitate straightforward installation and removal. Moreover, device alignment with respect to the MSSB will be improved by implementing a fully adjustable support structure, thereby improving magnet protection and minimising beam losses, see Fig.3.

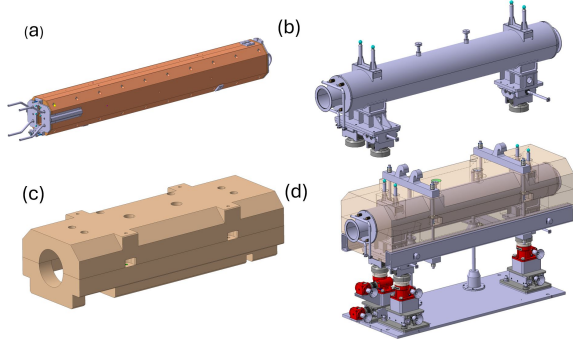


Figure 3: TCSC schematic illustration, where (a): CuCr1Zr core, (b): stainless steel vacuum chamber, (c): marble radiation shielding, and (d): full assembly on support structure.

## CORE MANUFACTURING

Each half of the core consists of an assembly joined by Hot Isostatic Pressing (HIP). It consists of two separate three-dimensionally forged CuCr1Zr blanks with a bent stainless-steel 316L cooling pipe positioned within machined grooves in the individual blanks. To ensure proper diffusion bonding, the HIP assembly is sealed using electron beam welding, and air is removed from the interfaces through a vacuum pinch-off (Fig. 4). By applying temperatures of up to approximately 950 °C and argon pressures reaching up to 100 MPa, strong metallurgical bonds are formed at the interfaces between the stainless-steel cooling tubes and the CuCr1Zr alloy. Under these conditions extensive tests have shown the effective elimination of thermal contact resistance between these two alloys, maximising cooling efficiency [4, 5].

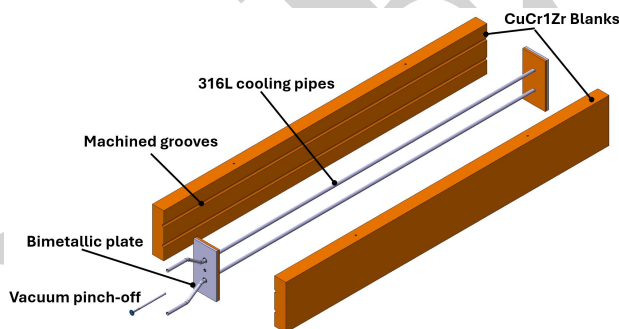


Figure 4: The stainless steel cooling pipes are positioned in precision-machined grooves in both CuCr1Zr blanks.

To recover the structural and thermal properties lost during the HIP-process, a subsequent heat treatment is performed

to each bonded assembly, including solution annealing, water quenching and precipitation hardening. The diffusion-bonded and heat-treated assemblies are then machined into their final shape, including a high control of the surface flatness over the length of the wedge contour providing the devices protective function. After the machining operations on either half of the core, both sides are bolted together.

The manufacturing tolerances were specified to ensure a small remaining gap with a nominal width of 74  $\mu\text{m}$  between both wedges, after bolting the two halves of the core together. This clearance accommodates thermal expansion of the wedges during beam interception and thereby reduces contact-induced stresses between the individual wedges.

## THERMOMECHANICAL RESPONSE

To assess the TCSC's structural and thermal performance under various conditions, finite element analysis was performed in ANSYS® [6] by using the energy deposition maps provided by FLUKA [7]. Transient thermal and quasi-static structural simulations were developed using temperature-dependent material models.

### Beam Parameters

Until LS3, both TCSCs are used only to split the slowly extracted shared beam (SFTPRO). However, in future operation one of the devices will also accommodate a dedicated beam for the Search for Hidden Particles (SHIP) experiment [8, 9]. This beam (SFTSHIP) will pass through the lower aperture of the TCSC without interacting with the device core, see Fig.5. In normal operation, neither TCSC is supposed to interact with this focused and highly energetic beam. The shared beam and dedicated beam use different optics and extraction cycles, see Table 1.

Table 1: Considered beam parameters for the shared and dedicated beams for future North Area operation [10].

Parameter	SFTPRO	SFTSHIP
Beam intensity [ $p/\text{pulse}$ ]	$4 \times 10^{13}$	$4 \times 10^{13}$
Cycle duration [s]	14.4	7.2
$p$ Momentum [GeV/c]	400	400
$\sigma_x, \sigma_y$ [mm]	1.13, 17.3	1.27, 1.24

### Operational and Accidental Scenarios

In previous operation, the TCSCs experienced misalignment of the SFTPRO beam relative to the wedges located at the centre of the core. This effect is therefore taken into account in the thermomechanical design. A conservative horizontal beam offset of up to 5 mm is considered as part of the operational conditions. Under normal operating conditions, the TCSCs reach thermal steady state after intercepting multiple beams. To evaluate the resulting thermal gradients and the associated beam-induced stress levels, this elevated steady-state temperature is used as the initial condition, after which a single additional beam is imposed.

Accidental scenarios include vertical and horizontal offsets of the SFTPRO beam of up to 20 mm, leading to significantly increased energy deposition, as well as an unintended

centred impact of the SFTSHIP beam on the TCSC, see Fig.5. During the simulated accidental cases, the TCSC is assumed to be at ambient temperature when a single beam is partially intercepted by the device.

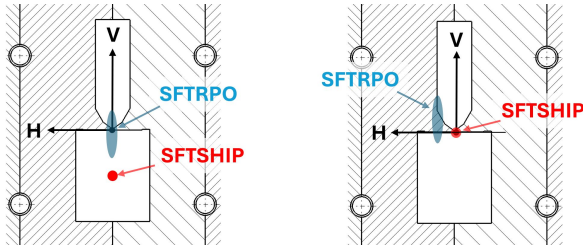


Figure 5: Visual representation of beam positions on the TCSC core cross section. Left: during nominal operation. Right: during accidental cases; SFTPRO horizontal (H) and vertical (V) misalignment and a centred SFTSHIP beam impact.

It must be mentioned that the North Area’s consolidated beam interlock systems (BIS), will be able to detect beam losses rapidly enough to prevent a full spill being deposited into TCSC under such accidental conditions by causing a beam dump [11].

### Cooling Conditions

It is conservatively assumed that all the heat deposited in the core is removed by the cooling water. The coolant’s heat transfer coefficient obtained from the Colburn equation [12] is approximately 2500 W/(m<sup>2</sup>K). The thermal contact conductance between the cooling pipes and the CuCr1Zr core is assumed infinite, as the thermal resistance in the contact is virtually eliminated via the diffusion bonding process. The simulations show minimal heat transfer between the bolted core halves, as the cooling pipes are located close to the beam energy deposition regions, enabling efficient local heat dissipation. The vacuum chamber is surrounded by a marble shielding structure. Since the air in the gap may be stagnant, a conservative heat transfer coefficient value of 0.5 W/(m<sup>2</sup>K) is applied on the lateral surface of the vacuum chamber.

### Simulation Results

Due to the strong convergence of the wedge shape, a significantly larger portion of the beam is absorbed in a single wedge in cases of misalignment, resulting in significantly higher temperatures and beam induced stresses as visualised in Fig.6. Under nominal operating conditions, maximum equivalent stresses of 24 MPa are observed for a perfectly aligned beam and 212 MPa for a horizontal misalignment of 5 mm. The corresponding occurring temperatures, as shown in Table 2, stay well below the service temperature of CuCr1Zr. Under these conditions, temperatures reach up to 308 °C, at which the yield strength of CuCr1Zr is significantly reduced. As a result, a local accumulated equivalent plastic strain of approximately 4.5% develops in the wedge. This value remains below the rupture strain of the alloy.

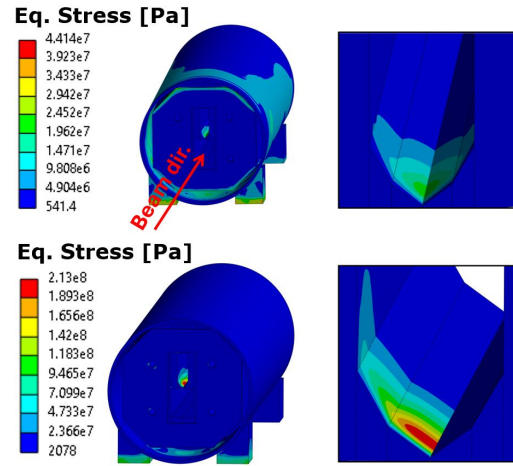


Figure 6: Top: Simulated stress-plot and wedge detail for a perfectly centred SFTPRO beam. Bottom: Simulated stress-plot for a 5 mm beam offset of an SFTPRO beam.

An unintended impact of the SFTSHIP beam results in accumulated plastic strains of up to 0.4%. In both accidental cases, the plastic deformation remains confined to a small volume of the wedge. Following a single such event, the device is expected to remain operational with only minor impact on its functionality and structural integrity.

Table 2: Simulated wedge stresses and temperatures due to an intercepted portion of primaries (pp) in operational and accidental cases.

Mode	Beam Type	Offset H,V [mm]	pp lost on TCSC [%]	Max Eq. Stress [MPa]	Max T [°C]
Oper.	SFTPRO	0,0	3	24	40
	SFTPRO	5,0	10	212	160
Acc.	SFTPRO	20,20	88	308	380
	SFTSHIP	0,0	20	258	400

### Device Monitoring

To validate and monitor the thermal performance of the next generation of TCSCs, two pairs of thermocouples will be installed in each device. These sensors will also aid in the detection of misalignment, which would result in an asymmetrical measured temperature profile.

## CONCLUSION

During LS3, two redesigned TCSCs will be installed in TT20 to improve reliability, cooling performance, and radiation safety. The upgraded design retains its crucial beam intercepting features while introducing HIP-bonded cooling channels, enhanced shielding, as well as improved accessibility and alignment features. The new TCSCs provide a robust and maintainable solution for future North Area operation, ensuring reliable beam splitting with reduced intervention time and personnel exposure.

## REFERENCES

- [1] D. Banerjee *et al.*, “The North Area at the CERN Super Proton Synchrotron”, CERN, Geneva, 2021, [doi:10.17181/CERN.GP3K.0S1Y](https://doi.org/10.17181/CERN.GP3K.0S1Y)
- [2] P. A. Arrutia Sota, *et al.* “TT20 Transport and Splitting of Beams Extracted Using Crystal Shadowing in LSS2 of the SPS”, CERN, Geneva, Switzerland, 20 Jul. 2020. <https://cds.cern.ch/record/2724487>
- [3] R. Franqueira Ximenes *et al.*, “Beam Intercepting Devices for the High Intensity Upgrade in CERN’s SPS North Area Facility”, Poster presented at the *8th High Power Targetry Workshop (HPTW2023)*, Wako, Japan, 7 Nov. 2023. <https://indico2.riken.jp/event/3102/contributions/21981/contribution.pdf>
- [4] A. Romero Francia *et al.*, “Design and early operation of a new-generation internal beam dump for CERN’s Super Proton Synchrotron”, *Phys. Rev. Accel. Beams* 27, 043001, 2024. [doi:10.1103/PhysRevAccelBeams.27.043001](https://doi.org/10.1103/PhysRevAccelBeams.27.043001)
- [5] S. Pianese *et al.*, “Hot isostatic pressing assisted diffusion bonding for application to the Super Proton Synchrotron internal beam dump at CERN”, *Phys. Rev. Accel. Beams* 24, 043001, 2021. [doi:10.1103/PhysRevAccelBeams.24.043001](https://doi.org/10.1103/PhysRevAccelBeams.24.043001)
- [6] ANSYS, Inc., ANSYS® Mechanical Enterprise™, version 2023 R2.
- [7] G. Battistoni *et al.*, “Overview of the FLUKA code”, *Annals of Nuclear Energy*, vol. 82, pp. 10-18, 2015. [doi:10.1016/j.anucene.2014.11.007](https://doi.org/10.1016/j.anucene.2014.11.007)
- [8] C. Ahdida *et al.*, “Findings of the Physics Beyond Colliders ECN3 Beam Delivery Task Force,”, *Journal of Physics G: Nuclear and Particle Physics*, vol. 47, no. 1, p. 010 501, 2019. [doi:10.1088/1361-6471/ab4cd2](https://doi.org/10.1088/1361-6471/ab4cd2)
- [9] SHiP Collaboration, “BDF/SHiP at the ECN3 high-intensity beam facility”, CERN, Geneva, Switzerland, Tech. Rep. CERN-SPSC-2022-032, Nov. 2022.
- [10] M. Fraser, “TCSC Beam Parameters”, Internal Design Review: TT20 TED, TBSE and TCSCs, CERN, Geneva, Switzerland, 26 Nov. 2024. Available: <https://indico.cern.ch/event/1476231/>
- [11] A. Colinet *et al.*, “The consolidation of the interlock systems for the CERN North Area”, in *Proc. IPAC’23*, Venice, Italy, May 2023, pp. 4101–4104. [doi:10.18429/JACoW-IPAC2023-THPA061](https://doi.org/10.18429/JACoW-IPAC2023-THPA061)
- [12] A. Colburn, “A method of correlating forced convection heat-transfer data and a comparison with fluid friction”, *International Journal of Heat and Mass Transfer*, vol 7, issue 12, 1964 [doi:10.1016/0017-9310\(64\)90125-5](https://doi.org/10.1016/0017-9310(64)90125-5)